Thermochimica Acta, 19 (1977) 287–300

A CALCULATION OF GIBBS FREE ENERGIES FOR FERROUS IONS AND THE SOLUBILITY OF MAGNETITE IN H_2O AND D_2O TO 300 °C

PETER R. TREMAINE*, RUDI VON MASSOW AND G. R. SHIERMAN
Atomic Energy of Canada Limited, Whiteshell Nuclear Research Establishment, Pinawa, Manitoba (Canada)
(Received 17 August 1976)

ABSTRACT

Gibbs energy and entropy data for aqueous Fe^{2+}, $FeOH^+$, $HFeO_2^-$ and FeO_2^{2-} are critically reviewed. The most reliable values are used in a Criss–Cobble extrapolation to calculate Gibbs energies to 300 °C and, hence, the solubility of Fe_3O_4 in H_2O and D_2O as a function of the pH or pD at 25 °C. A set if Gibbs energies is presented which satisfies the Criss–Cobble entropy correspondence principle and which is consistent with both the reliable low-temperature thermodynamic data and all published high-temperature solubilities.

INTRODUCTION

A detailed and accurate description of the solubility properties of magnetite is essential for predicting corrosion product transport in the primary heat transport circuits of nuclear power reactors[1-5]. Because the magnetite dissolution reaction involves the reduction of Fe^{3+} to Fe^{2+}, the solubility varies with the concentration of hydrogen gas in the water. Only three studies have been reported in which the hydrogen concentration was carefully controlled: two at pH less than 10.5[6,7] and one at pH 12 and 13[8]. The results of these studies are somewhat contradictory and none agree with the solubilities calculated by Macdonald et al.[9] using a Criss–Cobble extrapolation of room temperature thermodynamic data.

In order to resolve these discrepancies, we have critically examined the thermodynamic data for the various ferrous ions and used the most reliable values to calculate the solubility of magnetite as a function of pH and temperature. The uncertainties in both the calculated and experimental solubilities have been carefully evaluated and are often large. As a result, a pragmatic approach was adopted in which the most reliable experimental solubilities were used to refine the calculations in order to predict the solubility behavior of

*To whom correspondence should be addressed.

magnetite at pH's where the experimental data are sparse or widely scattered. The free energy data derived from this fitting procedure were used to estimate solubility data for D_2O.

SOLUBILITY CALCULATIONS

A. Thermodynamic Data

Unless otherwise specified, free energies and entropies were taken from the recent NBS tables[10] and heat capacities from Wicks and Block's compilation[11]. Values for the ionic dissociation product of water, K_w, and for the apparent molal free energy of water under its own vapour pressure were taken from Olofsson and Hepler[12] and from Helgeson and Kirkham[13], respectively. The equilibrium vapour pressure of hydrogen over solutions at elevated temperatures was calculated from Himmelblau's data[14] on the assumption that the dissolved hydrogen concentration is that of a saturated solution at 25 °C. The only measured values for the dissociation constant of LiOH at high temperature[15] are completely inconsistent with the precise data below 50 °C, probably because of the difficulties in determining large dissociation constants by conductance methods[16,17]. The values for the LiOH dissociation constant used here were obtained by extrapolating the low-temperature data[18,19], assuming a constant entropy of reaction, 2.65 J mol^{-1}K^{-1}. They are listed in Table 1 along with other high-temperature data. HCl was assumed to be completely dissociated at all temperatures.

TABLE 1

DISSOCIATION CONSTANTS AND HYDROGEN PARTIAL PRESSURES

	25 °C	*60 °C*	*100°C*	*150°C*	*200 °C*	*250 °C*	*300 °C*
$K_w \times 10^{14}/(\text{mol kg}^{-1})^2$	1.002	9.25	54.2	228	449	637	500
$K_D \times 10^{14}/(\text{mol}/1.1117\ \text{kg})^2$	0.136	1.58	9.57	42.8	99.1	133	116
LiOH, $K_B/\text{mol kg}^{-1}$	0.64	0.69	0.74	0.80	0.85	0.89	0.92
P_{H_2}/MPa^a	0.10132	0.10994	0.09384	0.06943	0.04722	0.03032	0.01831

^{a} For a 7.786×10^{-4} aquamolal concentration.

High-temperature apparent molal Gibbs energies of formation for OH^- and the various ferrous ions were calculated from data at 25 °C using the Criss–Cobble principle[20,21] and methods identical to those in ref. 22. Following Macdonald[22], the Gibbs energies of the hydrogen ion were determined from the calculated values for OH^- using the experimental values for K_w and the Gibbs energy of water. By definition[13,22], apparent molal Gibbs energies of formation are identical to standard molal Gibbs energies except that the former refer to standard state elements at 25 °C, rather than at the temperature in question. Data for the various ionic species in D_2O were crudely estimated by assuming that the Gibbs energy and entropy of all species except D^+ were identical to the light water values, using the hypothetical aquamolal* reference state. This assumption is correct to within a few hundred joules at 25 °C for monatomic species[23] but may be less accurate at higher temperatures and for hydrolysed species. Value for D^+ were determined from the calculated free energies of OD^- using Shoesmith's[24] values for the ionization constant of D_2O, K_D. High temperature Gibbs energies for D_2O were calculated from the 25 °C heat capacity. This procedure has been used for H_2O[22] and introduces an error of less than 40 J which, for the D_2O calculations here, is insignificant.

Many different values for the free energies and hydrolysis constants of the ferrous ions have been reported[25-36] and the choice of data is therefore crucial to the solubility calculations. The most reliable values for the Gibbs energies and entropies at 25 °C are tabulated in Table 2 and the reasons for choosing them are presented below. The neutral species, $Fe(OH)_2$, was not included in the calculations because of a lack of data.

TABLE 2

STANDARD GIBBS ENERGIES AND ENTROPIES[a] FOR FERROUS IONS AT 25 °C

	'best' literature value		*Fitted to solubility data*	
	ΔG^o (kJ mol^{-1})	*S^o (J mol^{-1}K^{-1})*	*ΔG^o (kJ mol^{-1})*	*S^o (J mol^{-1}K^{-1})*
Fe^{2+}	− 91.2±2.0	−107± 4	− 91.21	−107
$FeOH^+$	−278 ±3	− 29±17	− 274.26	− 33
$HFeO_2^-$ [b]	−383 ±8	+ 42±21	− 376.35	+ 63
FeO_2^{2-} [b]	−301 ±8	− 98±21	−(301.2)	(− 98)

[a] Not to be confused with Criss–Cobble absolute entropies. [b] Based on ΔG^o ($Fe(OH)_2$, solid) = −492±4 kJ mol^{-1}.

Patrick and Thomson[25] demonstrated that the often quoted figure[26] of −84.9 kJ mol^{-1} for the Gibbs energy of Fe^{2+} was obtained by e.m.f. measurements in an electrochemical cell contaminated by traces of oxygen. In oxygen-free systems, e.m.f. measurements yielded a Gibbs energy of −78.9 or −92.0 kJ mol^{-1} depending on whether the iron electrode was prepared by the decomposition of iron carbonyl or by hydrogen reduction, respectively[25]. The latter results agree well with Hurlen's value[27], of −90.0 kJ mol^{-1}, also from a reduced iron electrode. More recently, Larson et al.[28] calculated a Gibbs energy of −91.2±2.0 kJ mol^{-1} by combining measured heats of solution with existing thermodynamic data. This value agrees with the results from reduced iron electrodes and, since it was obtained by an independent method, it was accepted as correct. Patrick and Thompson's more positive value was probably

*One mole solute per 55.51 moles of solvent and equal to one mol/kg for H_2O and one mol/1.1117 kg for D_2O.

due to incomplete dissolution of the initial oxide film on the electrodes prepared from iron carbonyl[25].

The tabulated values[10,29–36] for the Gibbs energy of $FeOH^{+}$ are calculated from hydrolysis studies on ferrous salt solutions or on saturated solutions of ferrous hydroxide. The principal errors in most recent work[29–32] appear to be due to oxygen contamination and/or hydrolysable impurities. Under the reported experimental conditions, both contaminants would cause the observed values of the hydrolysis constant, pK_1, to be low. Oxidation of the ferrous species lowers the apparent pK_1, either because hydrolysis of Fe^{3+} to the more stable $FeOH^{2+}$ lowers the pH[29–32], or because ferric hydroxide, which is essentially insoluble relative to ferrous hydroxide[30], forms as a precipitate[29–32]. Hydrolysable impurities lower the apparent pK_1 by decreasing the measured pH. The highest values for pK_1 in the literature are 9.5 ± 0.2 and 9.49 ± 0.08 reported by Hedstrom[33] and Mesmer[34], respectively. Taking Mesmer's value, the free energy of the hydrolysis of Fe^{2+} is $+54.2 \pm 0.5$ kJ mol^{-1} and, hence, the Gibbs energy of $FeOH^{+}$ is -274.1 ± 2.5 kJ mol^{-1}.

Gibbs energies for $HFeO_2^-$ and FeO_2^{2-} have been calculated from the hydrolysis constants of solid ferrous hydroxide[35,36]. Foster[37] has noted that the accepted value of -482 kJ mol^{-1} for solid ferrous hydroxide[38] is based on irreproducible e.m.f.s and suggested that the true free energy is more negative. A more reliable Gibbs energy can be calculated from Leussing and Kolthoff's hydrolysis constants[29] by assuming that their figure for pK_1 differs from Mesmer's slightly higher value[34] because of impurities, as discussed above. The effect of these impurities on their other hydrolysis constants can then be eliminated by using Mesmer's pK_1 to calculate the concentration of impurities in their system. From the corrected hydrolysis constants and the Gibbs energy[28] of Fe^{2+}, the Gibbs energy of formation of ferrous hydroxide is -492 ± 4 kJ mol^{-1}. This results yields standard free energies of -385 ± 4 kJ mol^{-1} for $HFeO_2^-$ from Shrager's hydrolysis constants[36], and -383 ± 8 kJ mol^{-1} and -300 ± 8 kJ mol^{-1} for $HFeO_2^-$ and FeO_2^{2-}, respectively, from Gayer and Woontner's data[35].

The most reliable standard entropy for Fe^{2+} at 25 °C[28,29] appears to be -107 ± 4 J mol^{-1} K^{-1}. This value yields a standard entropy for $FeOH^{+}$ of 3 ± 15 J mol^{-1}K^{-1}, when combined with Bolzan and Arvia's entropy of hydrolysis[31]. The only other value in the literature is -29 ± 17 J mol^{-1}K^{-1}, derived from Sweeton and Baes' magnetite solubility study. Bolzan and Arvia's data yields pK_1 values which are much too low, according to the criteria discussed previously. We, therefore, chose Sweeton and Baes value for the calculations, even though it is not truly independent of the experimental data. Standard entropies for $HFeO_2^-$ and FeO_2^{2-} were estimated from Connick and Powell's empirical expression[40] to be $+42 \pm 21$ J mol^{-1}K^{-1} and -98 ± 21 J mol^{-1}K^{-1}. The standard molal entropies here and in Table 1 should not be confused with the absolute entropies required for the Criss–Cobble extrapolation[20,21].

B. Solubilities

All the evidence to date[49] suggests that the principal species in aqueous solutions of magnetite are Fe^{2+} and its hydrolysis products $FeOH^{+}$, $Fe(OH)_2$, $HFeO_2^-$ and FeO_2^{2-}. Magnetite dissolves according to reactions of the type[6,9]:

$$Fe_3O_4+(6-3b)H^+ + H_2 = 3Fe(OH)_b^{(2-b)+} + (4-3b)H_2O \tag{1}$$

where $0 \leqslant b \leqslant 4$ and where $Fe(OH)_3^-$ and $Fe(OH^4)_2^-$ are the hydrated formulations of $HFeO_2^-$ and FeO_2^{2-}, respectively. The aquamolal saturation concentration, m_b, of each ferrous species can be calculated from the expression[9]:

$$\log(m_b \gamma_b) = \frac{1}{3}\left[\frac{-\Delta G_R^\circ}{2.3025\,RT} - (6-3b)\,pH_T + \log\left(\frac{P_{H_2}}{0.10132}\right)\right] \tag{2}$$

where ΔG_R° is the aquamolal Gibbs energy of the solvation reaction, pH_T is the high temperature pH of the saturated solution, and P_{H_2} is the partial pressure (*MPa*) over a solution at high temperature. Above about 50 °C, the single ion activity coefficient, γ, can be expressed by the two parameter Debye–Hückel formula[41]

$$\log \gamma = \frac{-Z^2 A I^{1/2}}{(1+BI^{1/2})} \tag{3}$$

in which Z is the ionic charge, A is the Debye-Hückel limiting law parameter and I is the ionic strength of the system. The parameter B approaches a value of 1.5 ± 0.2 above 125 °C but is species dependent at lower temperatures[41]. Because of hydrolysis, the value of pH_T depends on the final equilibrium concentrations of ions in the solution, as does the ionic strength. For this reason, iterative procedures are required to calculate high-temperature solubilities from eqns (2) and (3) as a function of the low-temperature pH.

To be consistent with the usual experimental arrangement[6,8,42], our calculations refer to situations in which an initial feed solution at 25 °C, whose pH is set with either HCl or LiOH, is exposed to magnetite at high temperature. The concentration of hydrogen is that of a saturated solution at 25 °C, 7.786×10^{-4} aquamolal, and is assumed to be temperature-independent so that P_{H_2} could be calculated from Henry's law[14]. For computational simplicity, eqn (2) was considered adequate for calculating the concentration of LiOH or HCl corresponding to a given pH in the feed solution. The high temperature feed pH was then calculated from the temperature variations of K_w and the LiOH dissociation constant. The final pH and concentration of each ferrous species in the saturated solution were determined from eqns (2) and (3) and the charge balance of the system using an iterative method.

RESULTS AND DISCUSSION

The extrapolated values of the apparent Gibbs energies are listed in Table 3. The results for H^+ differ from Macdonald's[9] because more recent va-

TABLE 3

APPARENT GIBBS ENERGIES OF FORMATION[a] (kJ mol^{-1})

	25 °C	60 °C	100 °C	150 °C	200 °C	250 °C	300 °C
Fe_3O_4	−1015.5	−1020.9	−1027.8	−1037.5	−1048.2	−1059.9	−1072.5
H_2	0	−4.627	−10.045	−16.990	−24.106	−31.375	−38.785
D_2	0	−5.127	−11.118	−18.780	−26.616	−34.605	−42.735
H_2O	−237.18	−239.77	−243.07	−247.66	−252.68	−258.10	−263.88
D_2O	−243.49	−246.31	−249.92	−254.94	−260.45	−266.41	−272.77
H^+	0	+0.623	+0.690	−0.305	−2.172	−4.565	−6.975
D^+	−1.339	−1.025	−0.774	−1.699	−3.577	−6.058	−8.920
OH^-, OD^-	−157.29	−157.36	−156.76	−155.11	−152.59	−149.28	−145.26
Fe^{2+}	−91.21	−86.41	−82.16	−78.74	−77.29	−77.88	−80.46
$FeOH^+$, $FeOD^+$	−274.26	−272.69	−271.90	−272.42	−274.53	−278.28	−283.65
$HFeO_2^-$, $DFeO_2^-$	−376.35	−378.84	−380.64	−381.17	−379.77	−376.60	−371.62
FeO_2^{2-}	−301.2	−298.0	−291.2	−278.6	−261.4	−239.2	−212.0

[a] Aquamolal reference state for dissolved species.

lues[12] for K_w were used. Also, we used the figure −47.2 for the Criss–Cobble "a" parameter for OH^- and simple anions at 300 °C instead of the tabulated value[21] which is apparently a typographical error. The Gibbs energies of the ferrous ions were calculated from the data in the last two columns in Table 2 which were chosen to fit the experimental solubilities as discussed below. The error limits correspond to the maximum and minimum values of the literature data in Table 2.

The calculated light water solubilities are plotted in Figs. 1–5 as a function of the 25 °C pH of the iron-free feed solution. The upper and lower curves show the maximum and minimum solubilities which can be calculated from the "best" literature data in Table 2. The large uncertainty in the high temperature solubilities is primarily because the room temperature entropies of $FeOH^+$ and $HFeO_2^-$ and the Gibbs energy of $HFeO_2^-$ are so poorly known. The difference between our results and Macdonald's[9] at low pH is due to his use of Patrick and Thompson's suspect value for the Gibbs energy of Fe^{2+}. The horizontal region between pH 5 and pH 9 occurs because the equilibrium pH of the saturated solutions is buffered by the hydrolysis of the ferrous species released by the magnetite. Below pH 12, the calculations can be compared to experimental data using NaOH as a base because the effect of LiOH association on the OH^- concentration is less than 1%. The experimental data in the figures were measured[6,8,42] at 7.786×10^{-4} mol H_2/kg and lie within the uncertainty of the calculations. Kanert et al.[8] and Hawton and von Massow[42] removed oxygen by bubbling hydrogen through the feed solution in a 50 l carboy for 2 h before use. Tests in our laboratory showed that very high hydrogen flow-rates are required to reduce the oxygen concentration below 10^{-6} mol kg^{-1} so that there is a definite possibility of oxygen contamination in both measurements. Hawton and von Massow's results near the solubility

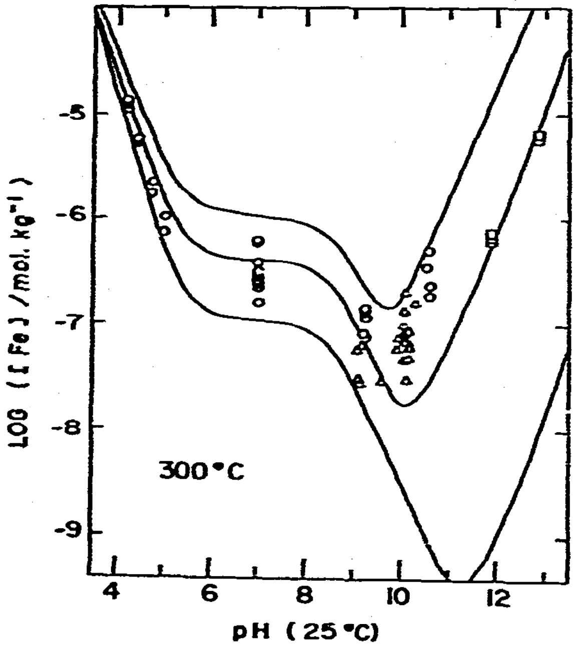

Fig. 1. Experimental and calculated solubilities of magnetite in H_2O at 300 °C plotted against the pH of the hydrogen saturated feed solution at 25 °C. The upper and lower curves are the maximum and minimum calculated solubilities. The middle curve is fitted to the data. O, ref. 6; □, ref. 8; Δ, ref. 42.

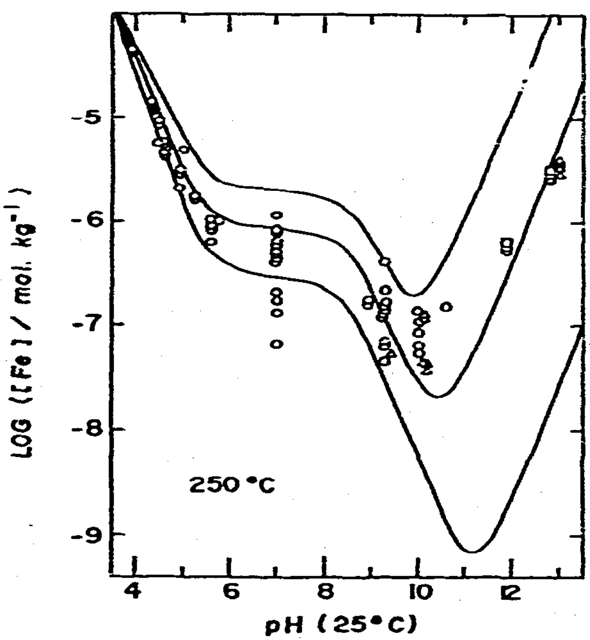

Fig. 2. The solubility of magnetite in H_2O at 250 °C. Description as in Fig. 1. Data from ref. 6 are at 260 °C.

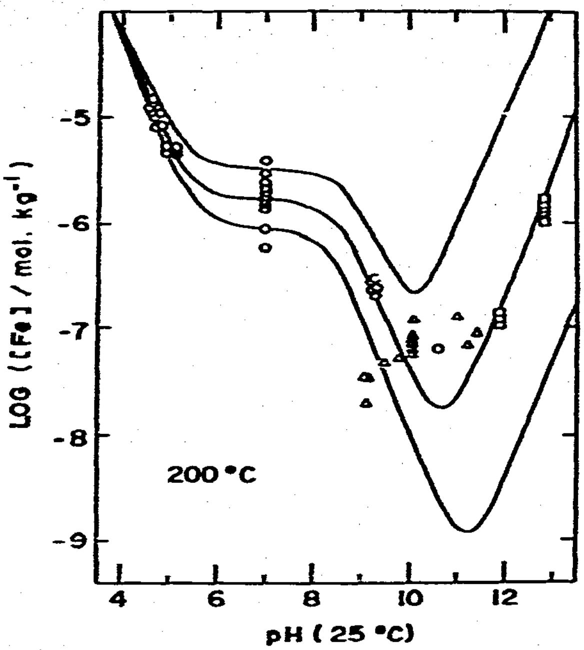

Fig. 3. The solubility of magnetite in H_2O at 200 °C. Description as in Fig. 1.

minimum are unreliable since their system may have contained residual iron. Their result at 250 °C and pH 12 agrees with Kanert et al. Sweeton and Baes[6] took scrupulous care to remove oxygen from their system but their results above pH 10 are few and scattered. The large scatter at pH 7 is undoubtably due to the effect of hydrolysable impurities on the high temperature pH.

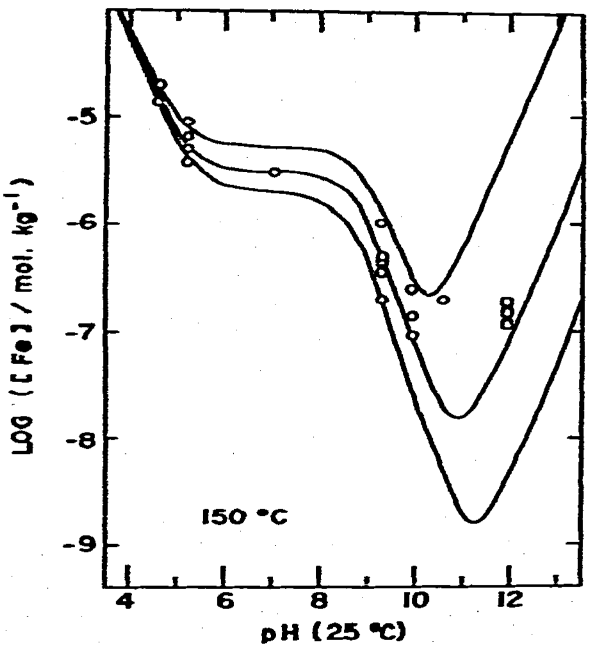

Fig. 4. The solubility of magnetite in H_2O at 150 °C. Description as in Fig. 1.

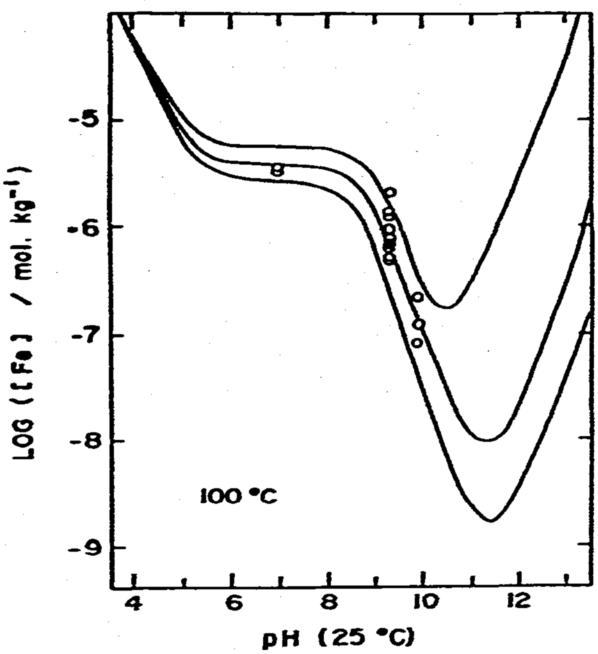

Fig. 5. The solubility of magnetite in H_2O at 100 °C. Description as in Fig. 1.

Obviously, neither the experimental nor the calculated data are accurate enough to describe the solubility over the entire pH and temperature range. A pragmatic approach to this problem is to use the experimental data to refine the calculations. We did this by choosing values for the room-temperature, thermodynamic parameters which lie within the error limits listed in Table 2 and which yield calculated high-temperature solubilities that agree with the reasonably precise results at pH<9.5 and pH>11.5. The result is shown in the middle curve in Figs. 1–5, obtained from the values in the last two columns in Table 2. The corresponding high temperature Gibbs energies are listed in Table 3. At 300 °C, and about pH 10.6, Sweeton and Baes' solubility results were higher than the trend of Kanert's data and we chose the latter for the fit because it was more precise and extended to high pH. The standard deviation of the experimental solubilities from refs 6 and 8 about the fitted curves was about 40 and 20%, respectively. From eqn (2), these standard deviations correspond to a precision of better than ± 2.5 kJ mol^{-1} for the high-temperature Gibbs energies for Fe^{2+}, $FeOH^+$ and $HFeO_2^-$ if the data for non-ferrous species are assumed to be exact. Below pH 14, FeO_2^{2-} did not contribute significantly to the solubility. The experimental results in the region of the solubility minimum are high, probably because of the presence of dissolved $Fe(OH)_2$, which was not considered in the calculation, or because of trace levels of iron in the apparatus. The data in Figs. 1–6 near the solubility minimum suggest that the concentration of $Fe(OH)_2$ is less than

2×10^{-7} mol kg^{-1} at high temperatures. Numerical values for the fitted solubilities are tabulated in Table 4.

Figure 6 shows the solubility data reported by Styrikovich et al.[7], along with the solubility curves calculated from the data in the last two columns of Table 2. Styrikovich saturated his solutions with hydrogen at high temperature and, for the solubility calculation, we assumed that the hydrogen pressure was the vapour pressure of water plus an overpressure of 0.1 MPa. At 285 °C, the experimental values below pH 4 lie within the 40% uncertainty in the calculated curve. The low experimental values between pH 4 and pH 9 are probably due to the effect of hydrolysable impurities on the high-temperature pH or to hydrogen leakage from the sealed autoclave. The discrepancy between the cal-

TABLE 4

THE CONCENTRATION OF IONIC FERROUS SPECIES IN SATURATED SOLUTIONS OF Fe_3O_4[a]

(A) Iron concentration in H_2O (mol kg^{-1})

ph	*25 °C*	*60 °C*	*100 °C*	*150 °C*	*200 °C*	*250 °C*	*300 °C*
3.0	5.2×10^{-4}	5.2×10^{-4}	5.2×10^{-4}	5.2×10^{-4}	5.1×10^{-4}	4.9×10^{-4}	4.6×10^{-4}
4.0	5.3×10^{-5}	5.3×10^{-5}	5.3×10^{-5}	5.2×10^{-5}	4.9×10^{-5}	4.2×10^{-5}	3.3×10^{-5}
5.0	7.6×10^{-6}	8.1×10^{-6}	7.9×10^{-6}	7.0×10^{-6}	5.4×10^{-6}	3.4×10^{-6}	2.1×10^{-6}
6.0	3.9×10^{-6}	4.4×10^{-6}	4.1×10^{-6}	3.2×10^{-6}	1.9×10^{-6}	1.0×10^{-6}	4.9×10^{-7}
7.0	3.6×10^{-6}	4.0×10^{-6}	3.8×10^{-6}	2.8×10^{-6}	1.7×10^{-6}	7.9×10^{-7}	4.0×10^{-7}
8.0	3.2×10^{-6}	3.7×10^{-6}	3.4×10^{-6}	2.5×10^{-6}	1.4×10^{-6}	6.5×10^{-7}	3.2×10^{-7}
9.0	1.2×10^{-6}	1.5×10^{-6}	1.4×10^{-6}	8.2×10^{-7}	3.9×10^{-7}	1.8×10^{-7}	8.4×10^{-8}
10.0	5.3×10^{-8}	7.6×10^{-8}	7.7×10^{-8}	5.6×10^{-8}	3.5×10^{-8}	2.2×10^{-8}	1.5×10^{-8}
11.0	4.3×10^{-9}	6.8×10^{-9}	8.9×10^{-9}	1.4×10^{-8}	2.4×10^{-8}	4.2×10^{-8}	6.2×10^{-8}
12.0	1.5×10^{-9}	6.2×10^{-9}	2.5×10^{-8}	9.1×10^{-8}	2.2×10^{-7}	4.3×10^{-7}	6.6×10^{-7}
13.0	2.9×10^{-8}	9.4×10^{-8}	3.2×10^{-7}	1.1×10^{-6}	2.8×10^{-6}	5.4×10^{-6}	8.3×10^{-6}
14.0	4.8×10^{-6}	9.3×10^{-6}	1.6×10^{-5}	3.1×10^{-5}	6.1×10^{-5}	1.1×10^{-4}	1.8×10^{-4}

B. Iron concentration in D_2O/(mol/1.1117 kg)

pD	*25 °C*	*60 °C*	*100 °C*	*150 °C*	*200 °C*	*250 °C*	*300 °C*
3.0	5.2×10^{-4}	5.2×10^{-4}	5.2×10^{-4}	5.2×10^{-4}	5.2×10^{-4}	5.1×10^{-4}	4.8×10^{-4}
4.0	5.1×10^{-5}	5.2×10^{-5}	5.2×10^{-5}	5.1×10^{-5}	5.0×10^{-5}	4.6×10^{-5}	4.0×10^{-5}
5.0	6.2×10^{-5}	6.4×10^{-6}	6.4×10^{-6}	6.0×10^{-6}	5.2×10^{-6}	4.0×10^{-6}	2.7×10^{-6}
6.0	2.3×10^{-6}	2.6×10^{-6}	2.4×10^{-6}	1.9×10^{-6}	1.3×10^{-6}	6.8×10^{-7}	3.3×10^{-7}
7.0	2.0×10^{-6}	2.2×10^{-6}	2.1×10^{-6}	1.6×10^{-6}	9.8×10^{-7}	4.7×10^{-7}	2.1×10^{-7}
8.0	1.9×10^{-6}	2.2×10^{-6}	2.0×10^{-6}	1.5×10^{-6}	9.1×10^{-7}	4.3×10^{-7}	1.9×10^{-7}
9.0	1.5×10^{-6}	1.8×10^{-6}	1.6×10^{-6}	1.2×10^{-6}	6.1×10^{-7}	2.6×10^{-7}	1.1×10^{-7}
10.0	1.7×10^{-7}	2.5×10^{-7}	2.2×10^{-7}	1.3×10^{-7}	6.4×10^{-8}	3.1×10^{-8}	1.5×10^{-8}
11.0	6.8×10^{-9}	1.0×10^{-8}	1.2×10^{-8}	1.0×10^{-8}	9.6×10^{-9}	1.1×10^{-8}	1.3×10^{-8}
12.0	9.0×10^{-10}	2.4×10^{-9}	6.7×10^{-9}	2.0×10^{-8}	4.5×10^{-8}	8.0×10^{-8}	1.2×10^{-7}
13.0	8.4×10^{-9}	2.2×10^{-8}	6.7×10^{-8}	2.1×10^{-7}	4.9×10^{-7}	8.7×10^{-7}	1.3×10^{-6}
14.0	1.2×10^{-6}	1.6×10^{-6}	2.0×10^{-6}	3.7×10^{-6}	6.9×10^{-6}	1.2×10^{-5}	1.7×10^{-5}

[a] pH and pD refer to a feed solution at 25 °C containing only LiOH or HCl and 7.786×10^{-4} aquamolal H_2 or D_2. (2) Near pH 7 the solubility would be affected by non ferrous hydrolysable ions. (3) The concentration of non-ionic species is probably less than 2×10^{-7} aquamolal and may be temperature dependent.

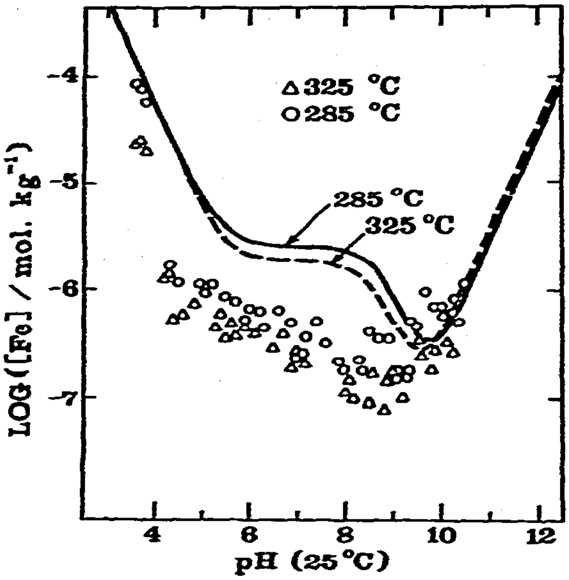

Fig. 6. Experimental and calculated solubilities of magnetite in H_2O at 285 °C with 7.01 *MPa* H_2 and at 325 °C with 12.16 *MPa* H_2. Experimental data from ref. 7.

culated and experimental results at 325 °C is due, at least in part, to our neglect of compressibility effects[43] which become important above 300 °C.

Sweeton and Baes' data at 300°C show a shap rise near pH 10 which is inconsistent with Kanert's results. Because of the experimental scatter, attempts to evaluate the concentrations of $Fe(OH)_2$ and $HFeO_2$ by curve fitting procedures must be based on high pH data, preferably above pH 12, where $HFeO_2$ is unquestionably the dominant species. For this reason, we used Kanert's results for the fitting and attributed the discrepancies at 300°C to statistical scatter. However, either the presence of dissolved oxygen or the formation of lithium ferrite[44,45] on the magnetite surface could have caused Kanert's results to be low and more experimental work in this high temperature–high pH region is clearly needed.

The solubility of magnetite in D_2O, calculated from the Gibbs energies in Table 3, is presented in Table 4. The difference in the solubilities at a given value for pH and pD is largely due to the stability of D_2O relative to H_2O (Table 3), since water occurs as a reagent or product in eqn (1). Because of the lack of high temperature data for ferrous systems in D_2O, it is impossible to estimate the accuracy of the calculated solubilities in Table 4. The largest uncertainty lies in our assumption that the replacement of OH groups by OD groups, with their different zero point energies[46], causes no marked changes in the Gibbs energies of the hydrolyzed ferrous species and OD^-. The data in Table 3 yield a value of 0.9 for ΔpK_1, the difference in the first hydrolysis constant of Fe^{2+} between D_2O and H_2O at 25 °C. This compares to values of ΔpK from 0.2 to 0.7 observed for most acids[46] at 25 °C. If the true value for

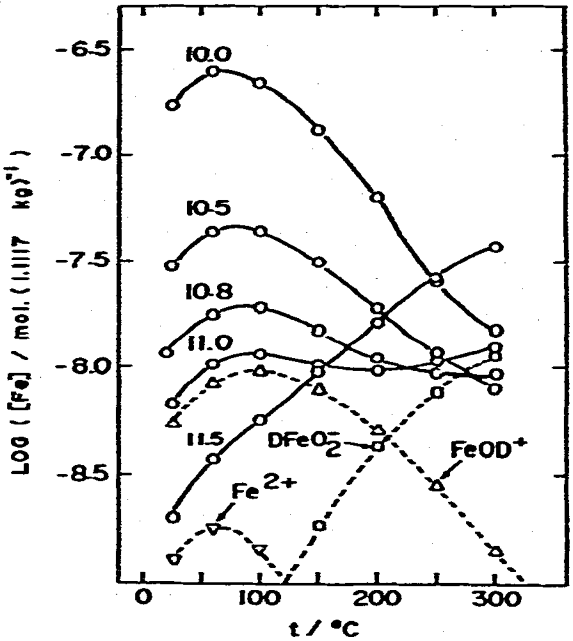

Fig. 7. Calculated solubilities of magnetite in D_2O as a function of temperature near the solubility minimum. The pD of the D_2 saturated 25 °C feed solution is shown above each curve. The broken lines show the contribution of $DFeO_2^-$ and $FeOD^+$ to the solubility at pD 11.0.

ΔpK_1 is in this range, then the sum $\Delta G^\circ(FeOD^+)+\Delta G^\circ(D^+)$ from Table 3 is too positive by 0.5 to 1.7 J mol^{-1} at 25 °C.

Figure 7 is a plot of the D_2O solubilities as a function of temperature for several values of pD near the solubility minimum. The marked change in the direction of the solubility–temperature gradient is caused by the increase in the concentration of $DFeO_2^-$ relative to $FeOD^+$ as the pD increases. The aquamolal concentrations of each species at pD 11.0 are shown by the broken lines. Heavy corrosion product deposits are thought to form on CANDU* reactor fuel bundles when the solubility at 300 °C is lower than that at 250 °C so that particulate deposits do not dissolve off the fuel[1–5]. Although the D_2O calculations indicate that this condition is met for $pD \geqslant 10.9$, CANDU reactors function successfully[47] at $pD \geqslant 10.4$. The calculated solubilities do not consider the contribution of neutral species, most probably $Fe(OD)_2$, to the overall solubility. If this is the major cause of the discrepancy, the difference in the concentration of $Fe(OD)_2$ between 300 °C and 250 °C is at least 5×10^{-9} mol/1.1117 kg.

CONCLUSIONS

Although the accuracy of Criss-Cobble extrapolations from 25 °C to temperatures above 200 °C has been questioned[48], the correspondence principle

*Canada Deuterium Uranium.

can be used as a convenient framework for correlating scattered high- and low-temperature results. Below pH 9.5, the magnetite solubilities and ferrous ion Gibbs energies reported here agree with all published solubility data and with the most reliable low-temperature data to within the experimental error. The results at higher pH are more suspect because of ambiguities in the experimental data on which the calculations were based. It is interesting to note the buffering effect of the magnetite dissolution reactions on feed solutions between pH 5 and 9. Many solubility studies on sparingly soluble oxides and metals are done using nominally neutral feed solutions in whicn the final high-temperature pH is unknown because it is determined by the hydrolysis reactions of the various system components. Thermodynamically meaningful solubilities cannot, therefore, be measured using neutral solutions unless the chemistry of the entire system is carefully defined.

Listings of the individual ion concentrations and activities corresponding to the solubilities in Table 4 and the details of the solubility calculations may be obtained from the authors upon request.

ACKNOWLEDGMENTS

We are indebted to Dr. D. W. Shoesmith and Prof. L. G. Hepler for their comments and suggestions.

REFERENCES

1 D. D. Macdonald, T. E. Rummery and M. Tomlinson, *Thermodynamics of Nuclear Materials 1974*, Vol. 2, International Atomic Energy Agency, Vienna, 1975, p. 123.
2 D. H. Lister, *Nucl. Sci. Eng.*, 58 (1975) 239.
3 M. Tomlinson, *Proceedings, International Conference on High Temperature High Pressure Electrochemistry in Aqueous Solutions, Surrey, U.K., 1973*, National Association of Corrosion Engineers, to be published.
4 M. Tomlinson, in M. Tomlinson (Ed.), *Activity Transport in Candus*, Atomic Energy of Canada Ltd., Report AECL-5113, 1975, p. 31.
5 B. Montford and T. E. Rummery, *Properties of Douglas Point Generating Station Heat Transport Corrosion Products*, Atomic Energy of Canada Ltd., Report AECL-4444, 1975.
6 F. H. Sweeton and C. F. Baes, *J. Chem. Thermodyn.*, 2 (1970) 479.
7 M. A. Styrikovich, O. F. Martynova, I. F. Kobyakov, V. L. Men'skikova and M. I. Reznikov, *Therm. Eng.*, 19 (1972) 127.
8 G. A. Kanert, G. W. Gray and W. G. Baldwin, *The Solubility of Magnetite in Basic Solutions at Elevated Temperatures*, Atomic Energy of Canada Ltd., Report AECL 5528, 1976.
9 D. D. Macdonald, G. R. Shierman and P. Butler, *The Thermodynamics of Metal–Water Systems at Elevated Temperatures 2: The Iron Water System*, Atomic Energy of Canada Ltd. Report, AECL-4137, 1972.
10 D. D. Wagman, W. H. Evans, V. B. Parker, I. Halow, S. M. Bailey and R. H. Schumm, *Selected Values of Chemical Thermodynamic Properties*, N.B.S. Technical Notes 270–3, 1968; and 270–4, 1969.
11 C. E. Wicks and F. E. Block, *U.S. Bur. Mines Bull.*, (1960) 605.
12 G. Olofsson and L. G. Hepler, *J. Solut. Chem.*, 4 (1975) 127.
13 H. C. Helgeson and D. H. Kirkham, *Am. J. Sci.*, 274 (1974) 1089.
14 D. M. Himmelblau, *J. Chem. Eng. Data*, 5 (1960) 10.

15 J. M. Wright, W. T. Lindsay and T. R. Druga, Westinghouse Electric Corp. WAPD-TM-204, 1961.
16 C. B. Monk, *Electrolytic Dissociation*, Academic Press, London, 1961, Ch. 8.
17 M. Spiro, *Trans. Faraday Soc.*, 55 (1959) 1746.
18 F. G. R. Gimblett and C. B. Monk, *Trans. Faraday Soc.*, 50 (1964) 965.
19 H. Ohtaki, *Acta Chem. Scand.*, 18 (1964) 521.
20 C. M. Criss and J. W. Cobble, *J. Am. Chem. Soc.*, 86 (1964) 5385.
21 C. M. Criss and J. W. Cobble, *J. Am. Chem. Soc.*, 86 (1964) 5390.
22 D. D. Macdonald and P. Butler, *Corrosion Sci.*, 13 (1973) 259.
23 E. M. Arnett and D. R. McKelvey, in J. F. Coetzee and C. D. Ritchie (Eds.), *Solute–Solvent Interactions*, Marcel Dekker, New York, 1969.
24 D. W. Shoesmith and W. Lee, *Can. J. Chem.*, in press.
25 W. A. Patrick and W. E. Thompson, *J. Am. Chem. Soc.*, 75 (1953) 1184.
26 W. M. Latimer, *The Oxidation States of the Elements and Their Potentials in Aqueous Solutions*, Prentice Hall, New Jersey, 2nd ed., 1952.
27 T. Hurlen, *Acta Chem. Scand.*, 14 (1960) 1533.
28 J. W. Larson, P. Cerutti, H. K. Garber and L. Helper, *J. Phys. Chem.*, 72 (1968) 2902.
29 D. L. Leussing and I. M. Kolthoff, *J. Am. Chem. Soc.*, 75 (1953) 2476.
30 K. H. Gayer and L. Woontner, *J. Am. Chem. Soc.*, 78 (1956) 3944.
31 J. A. Bolzan and A. J. Arvia, *Electrochim. Acta*, 8 (1963) 375.
32 J. Dauphin, S. Dauphin, D. Chatonier and Guy Andraud, *Bull. Soc. Chim. Fr.*, (1963) 2751.
33 B. O. A. Hedstrom, *Ark. Kemi*, 5 (1953) 457.
34 R. E. Mesmer, *Inorg. Chem.*, 10 (1971) 857.
35 K. H. Gayer and L. Woontner, *J. Phys. Chem.*, 60 (1956) 1569.
36 B. Schrager, *Chem. News*, 138 (1929) 354.
37 P. K. Foster, *New Zealand J. Sci.*, 2 (1959) 422.
38 M. Randall and M. Frandsen, *J. Am. Chem. Soc.*, 54 (1932) 47.
39 H. C. Ko and L. G. Hepler, *J. Chem. Eng. Data*, 8 (1963) 59.
40 R. E. Connick and R. E. Powell, *J. Chem. Phys.*, 21 (1953) 2206.
41 W. L. Marshall and E. V. Jones, *J. Phys. Chem.*, 70 (1966) 4028.
42 J. Hawton and R. von Massow, internal report, Whiteshell Nuclear Research Establishment, Atomic Energy of Canada Ltd.
43 J. W. Cobble, *J. Am. Chem. Soc.*, 86 (1964) 5394.
44 D. D. Macdonald and T. E. Rummery, *Corrosion Sci.*, 15 (1975) 521.
45 M. C. Bloom, M. Krulfeld and W. A. Fraser, *Corrosion*, 19 (1963) 327t.
46 P. M. Laughton and R. E. Robertson, in J. F. Coetzee and C. D. Ritchie (Eds.), *Solute–Solvent Interactions*, Marcel Dekker, New York, 1969.
47 R. L. Hemmings and D. Barber, in M. Tomlinson (Ed.), *Activity Transport in Candus*, Atomic Energy of Canada Ltd., Report AECL-5113, 1975, p. 17.
48 D. D. Macdonald, in B. E. Conway and J. O'M. Bockris (Eds.), *Modern Aspects of Electrochemistry*, Vol. 11, Plenum, New York, 1975, p. 141.
49 C. F. Baes, Jr. and R. E. Mesmer, *The Hydrolysis of Cations*, Wiley, New York, 1976.